Volume 19, Issue 5
October 2025

38 articles in this issue

Simple Optical Layout with a Diamond Crystal Monochromator for X-ray Spectromicroscopy

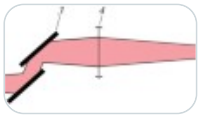

OriginalPaper | 26 January 2026 | Pages: 1065 - 1072

Nondestructive Determination of Qualitative and Quantitative Parameters of Coatings Based on Reflected Electron Spectroscopy

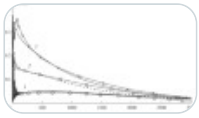

OriginalPaper | 26 January 2026 | Pages: 1073 - 1079

Formation and Relaxation of Elastic Stress in Radial InAs/InP Nanoheterostructures

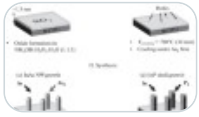

OriginalPaper | 26 January 2026 | Pages: 1080 - 1087

Numerical Study of Second Harmonic Generation in GaP Optical Nanoresonators

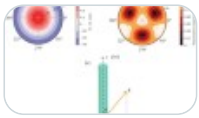

OriginalPaper | 26 January 2026 | Pages: 1088 - 1093

Formation of Nanoporous Germanium Layers by Irradiation with Indium Ions

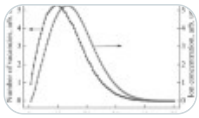

OriginalPaper | 26 January 2026 | Pages: 1094 - 1100

Investigation of Deuterium Saturation of a Polycrystalline Diamond Target at the HELIS Ion Accelerator

OriginalPaper | 26 January 2026 | Pages: 1101 - 1106

Effect of Low-Temperature Annealing on Magnetic Characteristics and Their Uniformity in Cobalt-Based Amorphous Alloy

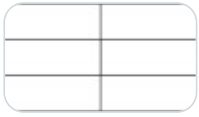

OriginalPaper | 26 January 2026 | Pages: 1107 - 1118

Kinetics of Changes in Optical Properties upon Electron Irradiation of $CaSiO_3$ Powder Modified with CeO_2 Nanoparticles

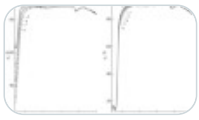

OriginalPaper | 26 January 2026 | Pages: 1119 - 1123

X-ray Structural Analysis of Core–Shell GaPNAs/GaP Nanowires Grown on a Si(111) Substrate

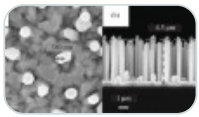

OriginalPaper | 26 January 2026 | Pages: 1124 - 1129

Study of Combined Effect of Helium Ion Implantation and Pulsed Laser Radiation on the Structure and Microhardness of the Surface of V–10Ti–6Cr–0.05Zr–0.1Si Alloy

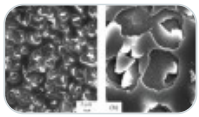

OriginalPaper | 26 January 2026 | Pages: 1130 - 1136

On the Effect of Weak Magnetic Fields on Electroplasticity and Microhardness of Zn–Al–Cu–Mg Alloy

OriginalPaper | 26 January 2026 | Pages: 1137 - 1140

Application of Synchrotron Radiation for Phase Analysis of Metal-Ceramic Materials Obtained by Laser Additive Manufacturing

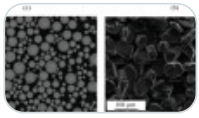

OriginalPaper | 26 January 2026 | Pages: 1141 - 1147

Design and Technological Solution Providing Temperature Self-Compensation of Thin-Film Chip Resistors

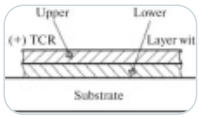

OriginalPaper | 26 January 2026 | Pages: 1148 - 1153

Surface Integrity and Fatigue Performance of Laser Shock Peened VT6 Titanium Alloy

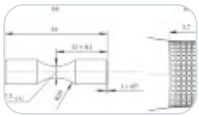

OriginalPaper | 26 January 2026 | Pages: 1154 - 1161

Synthesis of NiO [111] Thin Films on *c*-Al_2O_3 Substrates by Pulsed Laser Deposition

OriginalPaper | 26 January 2026 | Pages: 1162 - 1166

Transversal Motion Quantum States Populating in Planar Channeling Mode and the Resonant Capture of Relativistic Electrons in the Axial Channeling Mode

OriginalPaper | 26 January 2026 | Pages: 1167 - 1170

Determination of the Optimal Wavelength Range for Non-Contact Measurement of Temperature and Emissivity by Multispectral Pyrometry

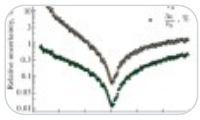

OriginalPaper | 26 January 2026 | Pages: 1171 - 1177

Deposition of Boron Carbide Films by Magnetron Sputtering of Powder and Solid B4C Targets

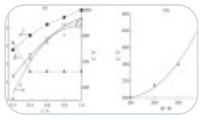

OriginalPaper | 26 January 2026 | Pages: 1178 - 1184

Pulsed Laser Deposition of Large-Area Molybdenum Disulfide Thin Films for THz Applications

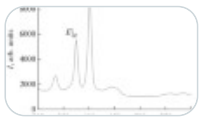

OriginalPaper | 26 January 2026 | Pages: 1185 - 1190

Excitation of Pulsed Cathodoluminescence by Picosecond Beams of Runaway Electrons

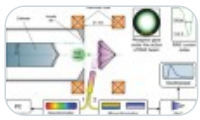

OriginalPaper | 26 January 2026 | Pages: 1191 - 1198

Effect of Equal-Channel Angular Pressing on Tribological Properties of AMg6 Alloy under Intense Sliding Friction

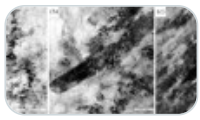

OriginalPaper | 26 January 2026 | Pages: 1199 - 1207

Deposition and Characterization of Nb–Ti Coating on Ti_6Al_4V Alloy

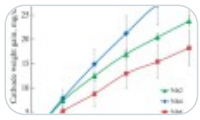

OriginalPaper | 26 January 2026 | Pages: 1208 - 1215

Modeling of Phase Composite Change of Ti–CuO Powder Mixture during Sintering Using Multistage Kinetics

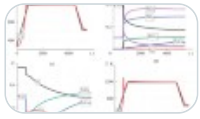

OriginalPaper | 26 January 2026 | Pages: 1216 - 1221

Ti_3SiC_2 MAX-Phase-Based Composites Produced by Vacuum and Spark Plasma Sintering

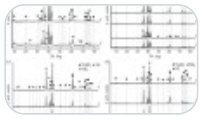

OriginalPaper | 26 January 2026 | Pages: 1222 - 1230

High-Temperature Oxidation of Laminated Ta/$Ti_3Al(Si)C_2$ Composites in the Temperature Range 800–1300°C

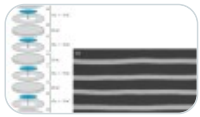

OriginalPaper | 26 January 2026 | Pages: 1231 - 1238

Analysis of Sorption and Desorption Characteristics of Nanolaminated Nb/Zr Systems

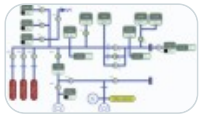

OriginalPaper | 26 January 2026 | Pages: 1239 - 1246

Thermal Diffusion of Cobalt in Iron Disilicide

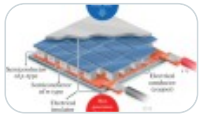

OriginalPaper | 26 January 2026 | Pages: 1247 - 1251

Orbital and Spin Quanta of Magnetic Flux

OriginalPaper | 26 January 2026 | Pages: 1252 - 1253

X-ray Photoelectron Spectroscopy Analysis of Changes in the Allotropic Structure of Samples of Tungsten and Carbon Subjected to Plasma Treatment

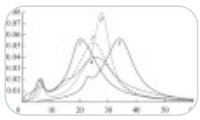

OriginalPaper | 26 January 2026 | Pages: 1254 - 1260

Investigation of Characteristics of Microparticles during Interaction of the Plasma Flow with the Surface of the Spacecraft during the Passage of the Atmosphere

OriginalPaper | 26 January 2026 | Pages: 1261 - 1271

Dynamic Mechanical Analysis of Viscoelastic Properties of Softwood and Hardwood as a Natural Polymer Material

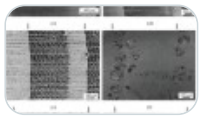

OriginalPaper | 26 January 2026 | Pages: 1272 - 1278

Application of Plasma Electrolytic Nitriding to Improve Wear Resistance of R6M5 High-Speed Steel

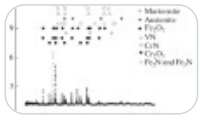

OriginalPaper | 26 January 2026 | Pages: 1279 - 1288

Exposure of Reduced Activation Ferritic/Martensitic Steels to Deuterium Plasma: a Review of Data on Surface Modification and Deuterium Diffusion and Accumulation

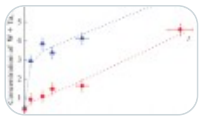

OriginalPaper | 26 January 2026 | Pages: 1289 - 1306

Features of Spectral-Temporal Analysis of Pulsed Emission from Stationary Plasma Thrusters

OriginalPaper | 26 January 2026 | Pages: 1307 - 1312

Arrangement of Catalytic Loops Correlated with Conenzyme Vibrations for Alcoholdehydrogenase Enzyme in Adsorption on a Carbon Surface

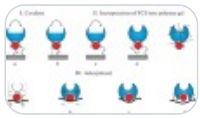

OriginalPaper | 26 January 2026 | Pages: 1313 - 1325

On one Method of Increasing the Resolution of X-Ray Diffraction Patterns

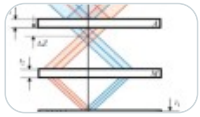

OriginalPaper | 26 January 2026 | Pages: 1326 - 1333

Combined Sintering of Yttrium Oxide-Stabilized Zirconium Dioxide Using Electron Beam Irradiation in the Forevacuum Pressure Region

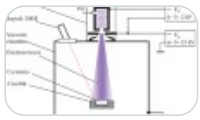

OriginalPaper | 26 January 2026 | Pages: 1334 - 1339

The Effect of Chemisorbed Quantum Dot Size at Graphene on the Charge Transfer

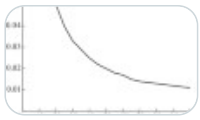

OriginalPaper | 26 January 2026 | Pages: 1340 - 1344